ISSN (Print) : 2320 – 3765
ISSN (Online): 2278 – 8875

International Journal of Advanced Research in Electrical, Electronics and Instrumentation Engineering

(An ISO 3297: 2007 Certified Organization)

Vol. 3, Issue 12, December 2014

Study of Kalman Filtering Techniques and Its Application for Optimal Power System Operation

K. Sowjanya, Prof., P.Sangameshwara Raju

Department of EEE, SV University, Tirupati, India

Department of EEE, SV University, Tirupati, India

ABSTRACT: Improve in power consumption cause serious balance issues in electrical power systems if there are no on-going or upcoming development tasks of new power plants or transmission lines. Additionally, such increase can result in large energy failures of the system. In expensive and ecologically effective way to prevent building the new infrastructures such as power plants, transmission lines, etc., the distributed generation (DG) has been compensated great attention.

KEYWORDS*:* Distributed generation, grid connection, Kalman filter algorithm, load-concentration-bus, optimal location, optimal size, power loss

I.INTRODUCTION

IN response to the recently improved prices of oil and natural gas, it is expected that the electrical energy industry will go through significant and fast change with regard to its framework, function, preparing, and control. Moreover, because of new restrictions placed by cost-effective, governmental, and ecological factors, styles in power system preparing and function are being forced toward maximum usage of current power facilities with limited working edges[2]. Therefore, the electrical powered power companies are attempting to achieve this purpose via many different ways, one of which is to delay the distribution generation (DG) remedy by a separate energy manufacturer (IPP) to meet growing customer fill demand. In this case, deferral attributes obtained by the IPP rely on the step-by-step system stability enhancement made by the DG remedy[1]-[4]. The DG is based on the alternative energy such as energy cell, photovoltaic or PV and wind energy as well as mixed heat and energy gas generator, micro-turbine, etc. Now, it becomes an essential important component of the modern energy system recently for several reasons.

II.ELECTION OF OPTIMAL LOCATIONS

A. Reduction of Power Loss by Connecting DG

In general, the presented power plants tend to be far from the consumption regions, and this situation causes a large amount of power loss on the power system. The IEEE benchmarked 30-bus system is shown in Fig. 1, The directly-connected-bus is defined as a bus connected to a location bus that does not pass through any other buses. For example, buses 12, 14, 18, and 23 in Fig. 1 are the directly-connected-buses if bus 15 is chosen as a reference bus. The load-concentration-bus handles relatively large loads, and Is more linked to the other directly-connected-buses when compared to other nearby buses. In Fig. 1, buses 10, 12, 27, and 5 can be selected as the delegate load-absorption buses of Areas 1 through 4, respectively.
Then, they provide an effect similar to the case where there are all DGs on each load bus, but with added benefit of reduced power loss From the Simplified unit circuit shown in Fig. 2, the power loss, P_{loss} between two buses, and , is computed by the following:

ISSN (Print) : 2320 – 3765
ISSN (Online): 2278 – 8875

International Journal of Advanced Research in Electrical, Electronics and Instrumentation Engineering

(An ISO 3297: 2007 Certified Organization)

Vol. 3, Issue 12, December 2014

$$P_{\text{loss},ij} = P_i - P_j = \frac{(P_i^2 + Q_i^2)\, r}{V_i^2}. \qquad (1)$$

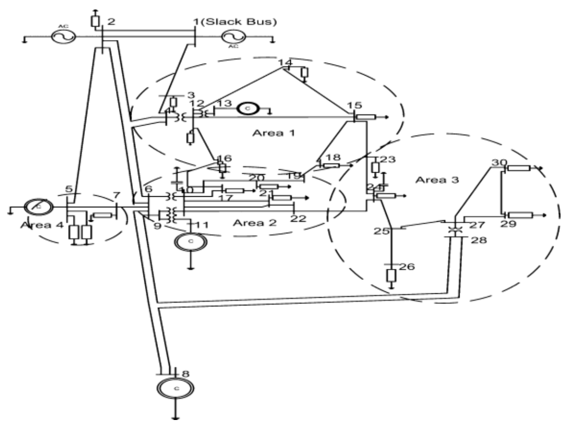

Fig1. IEEE benchmarked 30-bus system.

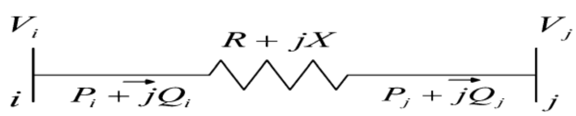

Fig2. Simplified unit circuit between two buses.

Also, the one-line plan of a distribution feeder with a total of n unit tour is proven in Fig. 3. When energy flows in one direction, the value of bus volt, V_{i+1}, has a smaller sized than that of V_i, and this associated formula can be indicated by (2).

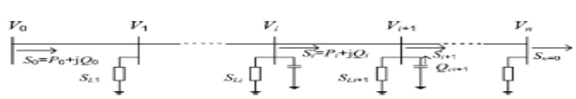

Fig3. One-line diagram of a distribution feeder.

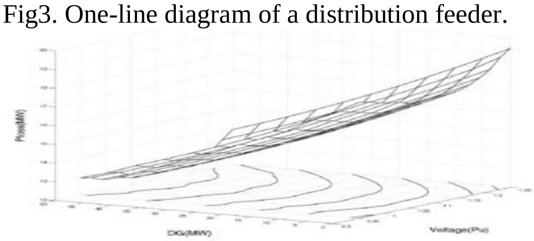

Fig4. Power loss corresponding to voltage and power of the DG.

ISSN (Print) : 2320 – 3765
ISSN (Online): 2278 – 8875

International Journal of Advanced Research in Electrical, Electronics and Instrumentation Engineering

(An ISO 3297: 2007 Certified Organization)

Vol. 3, Issue 12, December 2014

Earl, the reactive power Q_i, is decreased by linking a capacitor bank on bus in purchase to decrease the volts gap between V_{i+1} and V_i. In other terms, the capacitor financial institution at bus i creates it possible to decrease energy reduction and control the currents by adjusting the value of Q_i in the following:

$$V_{i+1}^2 = V_i^2 - 2(r_{i+1}P_i + x_{i+1}Q_i) + \left(r_{i+1}^2 + x_{i+1}^2\right)\left(P_i^2 + Q_i^2\right)/V_i^2. \quad (2)$$

If a DG is set up at the place of the capacitor financial institution, the proper delicate energy management of the DG has the same effect on the system as does the capacitor financial institution. Fig. 4 reveals the system power loss corresponding to the different energy and volts machines of the DG at the load-concentration-bus 10 in Place 2 of Fig. 1. It is noticed that the power loss is decreased almost linearly as the dimension DG improves.

B. Choice of Maximum Place for DGs by Considering Power Loss Before drawing the equations necessary to choose the optimal location for the DG, the following conditions is firstly defined.

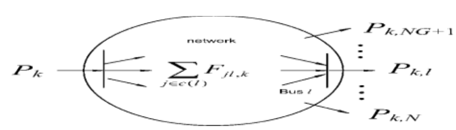

Fig5. Power flow from the kth generator to the loads

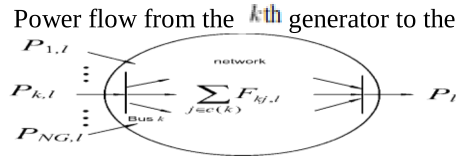

Fig6. Power flow from the several generators to the l load.

- $F_{jl,k}$: Power flowing from the kth generator to the lth load through bus j connected to the lth load;
- $D_{jl,k}$: Ratio of to the power supplied by the kth generator;
- $P_{loss,k}$: Power loss on transmission line due to the power supplied from kth generator;
- $F_{kj,l}$: Power flow from the kth generator to the lth load through bus j connected to the kth generator;
- $D_{kj,l}$: Ratio to the power supplied by the kth generator;
- $P_{loss,l}$: Power loss on a transmission line due to power supplied to the lth load;
- $p_{loss,i,j}$: Power loss between buses i and j;

The IEEE benchmarked 30-bus system in Fig. 1 is now analyzed for two different cases with respect to generator or load. In other words, the rest case is one where power flows from the kth generator to many loads. The first case is one where power is flowing from several generators to the lth load. These two surroundings are shown in Figs. 5 and 6, respectively. In First case power supplied from kth generator to the lth load among a number of loads is considered by the following:

$$P_{k,l\,|case-1} = \sum_{j\in c(l)} F_{jl,k} = \sum_{j\in c(l)} D_{jl,k}\, P_k \quad (3)$$

Where c(l) are the buses coupled to the lth load. Then power loss joint with the kth generator is designed by the following. Which is the differentiate between the power supplied from the kth generator and total power inspired in loads.

ISSN (Print) : 2320 – 3765
ISSN (Online): 2278 – 8875

International Journal of Advanced Research in Electrical, Electronics and Instrumentation Engineering

(An ISO 3297: 2007 Certified Organization)

Vol. 3, Issue 12, December 2014

$$P_{loss,k} = P_{k-}\sum_{l=NG+1}^{N} P_{k,l} \qquad (4)$$

Case-2 The power supplied from the kth generator to along with a number of generators to the lth load is designed.

$$P_{k,l\,|case-2} = \sum_{j\in c(k)} F_{kj,l} = \sum_{j\in c(k)} D_{kj,l}\, P_l \qquad (5)$$

Where c(k) are the buses coupled to the kth generator the power loss joint with the lth load is calculated by the following equation:

$$P_{loss,l} = \sum_{k=1}^{NG} P_{k,l_{P_l}} \qquad (6)$$

In a mixture of the situations described above, the power system in Fig. 1 can be indicated by total power loss shown in Fig. 7 with concern of only energy years and consumptions. The division between buses and in Fig. 7 can become an arbitrary division in Fig. 1. When the product routine of Fig. 2 is regarded, Fig. 8 reveals the difference of power loss corresponding to the dimension DG at load-concentration-bus 10 and the amount of fill intake at bus 21 in Fig. 1.

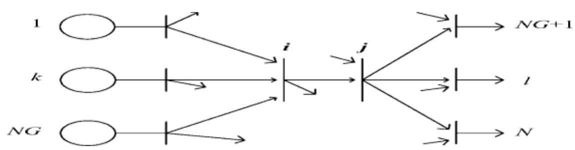

Fig7. Simplified circuit with only power generations and consumptions.

III.PROCEDURE TO SELECT OPTIMAL SIZE OF MULTIPLE DGS USING KALMAN FILTER ALGORITHM

The quantity of power consumption each area could be selected as the optimal values for the DGs to be placed. However, these are not maximum principles for the DGs because the power reduction in lines linking two buses is ignored. The Kalman filter criteria have the removing properties and the disturbance being rejected ability effective to the process and statistic sounds. In realistic surroundings (in which the declares are motivated by procedure disturbance and statement is made in the existence of statistic noise),

$$\begin{aligned} \mathbf{x}(n+1) &= \mathbf{\Phi}\mathbf{x}(n) + \mathbf{\Gamma}\boldsymbol{\omega}(n), \mathbf{x}(0) = \mathbf{x}_0 \\ y(n) &= \mathbf{c}\cdot\mathbf{x}(n) \\ z(n) &= y(n) + v(n) \end{aligned} \qquad (7)$$

Where the matrices, $\mathbf{\Phi}(\in \mathbf{R}^{n\times n})$ and, and the $\mathbf{\Gamma}(\in \mathbf{R}^{n\times m})$, vector, $\mathbf{c}(\in \mathbf{R}^{1\times n})$, are known deterministic variables, and the identity matrix, $\mathbf{I}(\in \mathbf{R}^{n\times n})$, is usually chosen for the matrix,. The state vector, $\mathbf{x}(\in \mathbf{R}^{n\times 1})$,, can represent the size of each of the multiple DGs or their coefficients. Also, $\boldsymbol{\omega}(\in \mathbf{R}^{m\times 1})$ is the process noise vector, is the measured power loss, and is stationary measurement noise. Then, the estimate of the state vector z is updated by using the following steps.

- **Measurement update:** Acquire the measurements, $z(n)$, , and compute *a posteriori* quantities:

$$\begin{aligned} \mathbf{k}(n) &= \mathbf{P}^-(n)\mathbf{c}^T[\mathbf{c}\mathbf{P}^-(n)\mathbf{c}^T + r]^{-1} \\ \hat{\mathbf{x}}(n) &= \hat{\mathbf{x}}^-(n) + \mathbf{k}(n)[z(n) - \mathbf{c}\hat{\mathbf{x}}^-(n)] \\ \mathbf{P}(n) &= \mathbf{P}^-(n) - \mathbf{k}(n)\mathbf{c}\mathbf{P}^-(n) \end{aligned} \qquad (8)$$

Where $\mathbf{k}(\in \mathbf{R}^{n\times 1})$ is the Kalman gain, $\mathbf{P}$ is a positive-definite symmetric matrix, and Is a positive number selected to avoid a singular matrix typically, $\mathbf{P}^-(0)$ is given as $\mathbf{P}^-(0) = \lambda\mathbf{I}(\lambda > 0)$, $\mathbf{I}$, where is an identity matrix.

$$\begin{aligned} \hat{\mathbf{x}}^-(n+1) &= \mathbf{\Phi}\hat{\mathbf{x}}(n) \\ \mathbf{P}^-(n+1) &= \mathbf{\Phi}\mathbf{P}(n)^T + \mathbf{\Gamma}\mathbf{Q}\mathbf{\Gamma}^T \end{aligned} \qquad (9)$$

Where $\mathbf{Q}(\in \mathbf{R}^{m\times m})$ is a positive-defined covariance matrix, which is zero in this study because the stationary process and measurement noises are mutually independent.

10.15662/ijareeie.2014.0310075

ISSN (Print) : 2320 – 3765
ISSN (Online): 2278 – 8875

International Journal of Advanced Research in Electrical, Electronics and Instrumentation Engineering

(An ISO 3297: 2007 Certified Organization)

Vol. 3, Issue 12, December 2014

Time increment: Increment n and repeat. Thereafter, the estimated output (the total power loss of the system) is calculated as

$$\hat{y}(n) = \mathbf{c}\hat{\mathbf{x}}(n). \qquad (10)$$

Fig. 9 shows the process to acquire information examples for the sizes of several DGs and the power reduction needed before applying the Kalman filter criteria. In Stage-1 of Fig. 9, the algorithm begins with the zero principles for all DGs, and the catalog signifies the number of given DG. Including the little bit of power, P_{step} of 10 MW to each DG, the preliminary power reduction is obtained by a energy flow calculations in accordance with the Newton–Raphson Method.

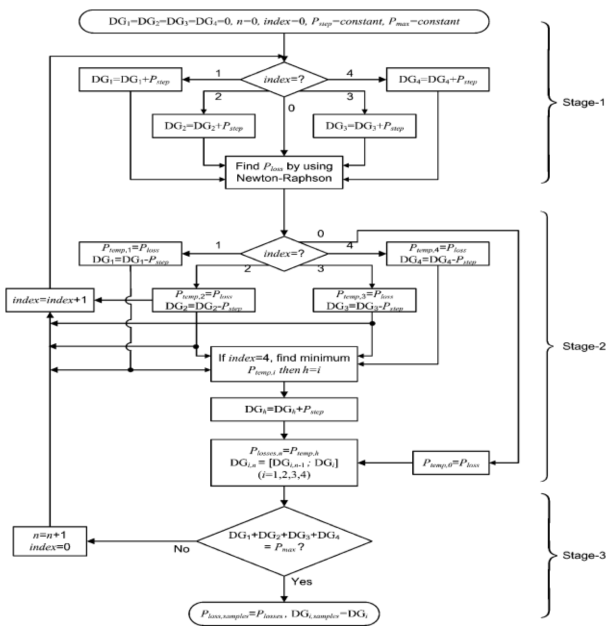

Fig.9. Procedure to obtain data samples of the Kalman filter algorithm

Then, the details on the person power loss, required before applying.

corresponding to each DG improved by 10 MW is sent to Stage-2, where the of P_{loss} are replaced with those of. After the lowest value of is P_{temp} chosen, its value and the corresponding dimensions of several DGs are saved in the memory of $P_{\text{losses},n}$ and DG in Fig. 9, respectively. This process is then recurring until the complete sum of all DGs is the same as the predefined value, $P_{\max}$, in Stage-3 by increasing n to $n+1$. . Finally, the accumulated data of the minimum power loss and sizes of DGs, which are $P_{\text{losses,samples}}$ and $\text{DG}_{i,\text{samples}}$, respectively, are obtained.

The information examples acquired above might be dissimilar from the real values due to the giant testing period of 10 MW. If this testing period is decreased to locate more precise principles, the computational need will be significantly improved.

In Phase-1 of Fig. 10, the anticipated sizes of multiple DGs, $\text{DG}_{i,\text{estimated}}$, are determined by applying the Kalman filter algorithm with the data samples obtained from Fig. 9, which are $P_{\text{losses,samples}}$ and $\text{DG}_{i,\text{samples}}$. and . Its associated parameters are then given in the following:

ISSN (Print) : 2320 – 3765
ISSN (Online): 2278 – 8875

International Journal of Advanced Research in Electrical, Electronics and Instrumentation Engineering

(An ISO 3297: 2007 Certified Organization)

Vol. 3, Issue 12, December 2014

$$\delta(n) = \sum_{i=1}^{4} \mathrm{DG}_{i,\mathrm{samples}}(n) / \max \times \left\{ \sum_{i=1}^{4} \mathrm{DG}_{i,\mathrm{samples}}(n) \right\} \quad (11)$$

$$\mathbf{c}_{\mathrm{Phase-1}}(n) = [\delta(n), \delta^2(n), \delta^3(n), \delta^4(n)] \quad (12)$$

$$z(n)|_i = \mathrm{DG}_{i,\mathrm{samples}}(n) \quad (13)$$

$$\mathrm{DG}_{i,\mathrm{estimated}}(n) = \hat{y}(n) = \mathbf{c}_{\mathrm{Phase-1}}(n) \cdot \hat{\mathbf{x}}_{\mathrm{Phase-1}}(n_{\max})|_i$$

$$(i = 1, 2, 3, 4) \quad (14)$$

Where δ is the normalize value, $n_{\max}$ and is the number of last samples in $\mathrm{DG}_{i,\mathrm{samples}}$. To approximation the size of each DG, the Kalman filter algorithm is useful in series with dissimilar dimensions of z in (13). After estimating the most favorable sizes of numerous DGs in Phase-1, the overall power loss, $P_{\mathrm{loss,estimated}}$, is estimated in Phase-2 of Fig. 10 with the power loss information samples, $P_{\mathrm{loss,samples}}$, from Fig. 9 and the estimated DG sizes, DG , in Phase-1. The coupled parameters required to apply the Kalman filter algorithm are given in the following:

$$\beta_i(n) = \mathrm{DG}_{i,\mathrm{estimated}}(n), \quad (i = 1, 2, 3, 4) \quad (15)$$

$$\mathbf{c}_{\mathrm{Phase-2}}(n) = [\beta_1(n), \beta_2(n), \beta_3(n), \beta_4(n)] \quad (16)$$

$$z(n) = P_{\mathrm{loss,samples}}(n) \quad (17)$$

$$P_{\mathrm{loss,estimated}}(n) = \hat{y}(n) = \mathbf{c}_{\mathrm{Phase-2}}(n) \cdot \hat{\mathbf{x}}_{\mathrm{Phase-2}}(n_{\max}) \quad (18)$$

Where β is the estimated size for each DG from (14).

Future scope:
In future we have to find out the cost function. Depending up on the cost function of dispatchable DGs used.

IV.SIMULATION RESULTS

Active power losses	Reactive power losses
1.907 Mw	10.827MVAR

Power losses

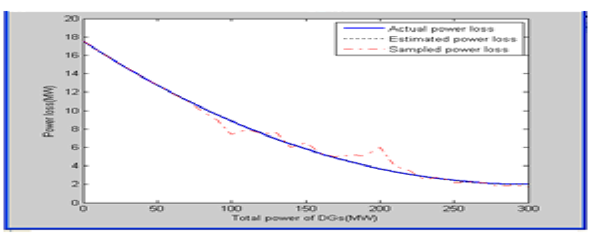

Estimation performance of total power loss.

V.CONCLUSION

This document suggested the means for choosing the maximum locations and sizes of multiple distributed generations (DGs) to minimize the complete power lack of system. To cope with this optimization problem, the Kalman filter criteria were used. When the maximum dimensions of several DGs are chosen, the computation efforts might be significantly improved with many data Samples from a large-scale power system because the entire system must be examined for each information example. The proposed procedure in accordance with the Kalman filter criteria took the only few examples, and therefore decreased the computational requirement dramatically during the marketing process.

ISSN (Print) : 2320 – 3765
ISSN (Online): 2278 – 8875

International Journal of Advanced Research in Electrical, Electronics and Instrumentation Engineering

(An ISO 3297: 2007 Certified Organization)

Vol. 3, Issue 12, December 2014

REFERENCES

[1] A. A. Chowdhury, S. K. Agarwal, and D. O. Koval, "Reliability modeling of distributed generation in conventional distribution systems planning and analysis," *IEEE Trans. Ind. Appl.*, vol. 39, no. 5, pp.1493–1498, Oct. 2003.
[2] M. F. AlHajri and M. E. El-Hawary, "Improving the voltage profiles of distribution networks using multiple distribution generation sources," in *Proc. IEEE Large Engineering Systems Conf. Power Engineering*, 2007, pp. 295–299.
[3] G. Carpinelli, G. Celli, S. Mocci, F. Pilo, and A. Russo, "Optimization of embedded generation sizing and siting by using a double trade-off method," *Proc. Inst. Elect. Eng., Gen., Transm., Distrib.*, vol. 152, no. 4, pp. 503–513, Jul. 2005.
[4] T. Senjyu, Y. Miyazato, A. Yona, N. Urasaki, and T. Funabashi, "Optimal distribution voltage control and coordination with distributed generation," *IEEE Trans. Power Del.*, vol. 23, no. 2, pp. 1236–1242, Apr. 2008.
[5] H. Saadat, *Power System Analysis*, 2nd ed. , Singapore: McGrawHill, 2004, pp. 234–227.
[6] J. J. Grainger and S. H. Lee, "Optimum size and location of shunt capacitors for reduction of losses on distribution feeders," *IEEE Trans. Power App. Syst.*, vol. PAS-100, no. 3, pp. 1105–1118, Mar. 1981.
[7] M. Baran and F. F. Wu, "Optimal sizing of capacitors placed on a radial distribution system," *IEEE Trans. Power Del.*, vol. 4, no. 1, pp. 735–743, Jan. 1989.
[8] M. A. Kashem, A. D. T. Le, M. Negnevitsky, and G. Ledwich, "Distributed generation for minimization of power losses in distribution systems," in *Proc. IEEE PES General Meeting*, 2006, pp. 1–8.

10.15662/ijareeie.2014.0310075